Cooperative Assembly of a Nativelike Ubiquitin Structure through Peptide Fragment Complexation: Energetics of Peptide Association and Folding[†]

Muriel Jourdan and Mark S. Searle*

Department of Chemistry, University of Nottingham, University Park, Nottingham NG7 2RD, United Kingdom

Received March 30, 2000; Revised Manuscript Received June 16, 2000

ABSTRACT: Peptide fragments corresponding to the N- and C-terminal portions of bovine ubiquitin, U(1−35) and U(36−76), are shown by NMR to associate in solution to form a complex of modest stability ($K_{assn} \approx 1.4 \times 10^5$ M^{-1} at pH 7.0), with NMR features characteristic of a nativelike structure. The complex undergoes cold denaturation, with temperature-dependent estimates of stability from NMR indicating a ΔC_p° for fragment complexation in good agreement with that determined for native ubiquitin, suggesting that fragment association results in the burial of a similar hydrophobic surface area. The stability of the complex shows appreciable pH dependence, suggesting that ionic interactions on the surface of the protein contribute significantly. However, denaturation studies of native ubiquitin in the presence of guanidine hydrochloride (Gdn·HCl) show little pH dependence, suggesting that ionic interactions may be "screened" by the denaturant, as recently suggested. Examination of the conformation of the isolated peptide fragments has shown evidence for a low population of nativelike structure in the N-terminal β-hairpin (residues 1−17) and weak nascent helical propensity in the helical fragment (residues 21−35). In contrast, the C-terminal peptide (36−76) shows evidence in aqueous solution, from some Hα chemical shifts, for nonnative ϕ and ψ angles; nonnative α-helical structure is readily induced in the presence of organic cosolvents, indicating that tertiary interactions in both native ubiquitin and the folded fragment complex strongly dictate its structural preference. The data suggest that the N-terminal fragment (1−35), where interaction between the helix and hairpin requires the minimum loss of conformational entropy, may provide the nucleation site for fragment complexation.

Current models for the mechanism of protein folding favor a hierarchical process in which folding begins at the local sequence level involving structural elements of marginal stability that interact, leading to ever-increasing levels of complexity, from which nativelike secondary structure and tertiary interactions emerge (*1*−*5*). Much evidence from peptides and denaturated states of proteins supports the suggestion that folding initiation is driven by local sequence information (*6*−*10*). These results suggest that peptide fragments ("microdomains") should possess the propensity to associate and assemble into a nativelike protein structure just as a single, contiguous polypeptide chain, despite the entropic cost of the bimolecular association. The association of peptide fragments to form a fully reconstituted nativelike protein structure, together with a detailed thermodynamic or kinetic analysis of the complexation process, has been described in detail for a handful of small proteins, showing that all the information required for noncovalent interactions in the native state is also available through the coalescence of largely disordered complementary fragments (*11*−*14*).

Folding studies with peptide fragments provide a highly complementary approach to examine current models for the mechanism of protein folding and for studying the energetics of protein−protein interactions and the nature of the weak interactions involved in the fragment recognition process (*15*). A further advantage is that individual fragments can be studied at equilibrium under folding conditions to detect evidence of local interactions within contiguous parts of the polypeptide chain that may provide the necessary nuclei for folding (*16, 17*). The observation that fragments are able to associate in a bimolecular process strongly supports the idea that these nucleation events are highly localized (*3*−*5*). For example, barnase is an $\alpha + \beta$ protein that has been studied by the fragment reconstitution approach. The elements of secondary structure of barnase are located in different halves of the polypeptide chain, enabling them to be separated in peptide fragments. Studies of the individual fragments show some evidence for a nativelike structural propensity that results in rapid folding (*11*). In contrast, chymotrypsin inhibitor 2 (CI-2) is an α/β protein in which the secondary structure is not clearly separated in the two fragments. The 25-fold slower association rate constant compared with barnase has been explained by the absence of well-defined initiation sites within each fragment even though the fragments associate tightly to form a stable complex (*13*).

Only a few studies to date have investigated in detail the energetics of the fragment complexation process (*14*). To this end, we have chosen bovine ubiquitin as a suitable model system. Ubiquitin is a small protein of 76 residues composed of a single domain whose folding pathway is not complicated

[†] We thank the BBSRC of the U.K. for financial support, the European Commission for a Marie Curie Research Fellowship to M.J., and the Department of Chemistry, University of Nottingham, and EPSRC for funding the NMR facilities.

* Corresponding author: Tel 0115 951 3567; fax 0115 951 3564; e-mail mark.searle@nottingham.ac.uk.

10.1021/bi000718r CCC: $19.00
Published on Web 09/12/2000

by disulfide bond formation or metal or cofactor binding. Its folding mechanism and stability have been well-studied by a variety of spectroscopic and calorimetric techniques (*18*−*23*) and hydrogen−deuterium exchange methods (*24*, *25*), while structural data are available from both NMR and X-ray crystallography (*26*−*28*). A partially unfolded state of ubiquitin (A-state) has been identified in aqueous methanol in which the N-terminal portion of the sequence (residues 1−35) appears to retain nativelike structure (*29*). Subsequently, NMR and CD studies of the folding of isolated peptide fragments from the N-terminal 35-residue portion of the sequence, including the β-hairpin (1−17) and hairpin−helix segment (1−35), have shown evidence for residual structure in aqueous methanol, suggesting these as possible folding nucleation sites (*30*). More recently, a small population of nativelike β-hairpin structure has been identified in fragment 1−17 in aqueous solution (*31*).

Toward understanding the mechanism and energetics of folding of ubiquitin, we describe the reconstitution of a nativelike structure from two peptide fragments, one corresponding to the N-terminal sequence U(1−35) and the other encompassing the remainder of the β-sheet and loop regions within the sequence U(36−76). The cleavage point between the two portions of the sequence is located in a solvent exposed loop at the C-terminal end of the first helix (between Gly35 and Ile36) in a position expected to have a minimal destabilizing effect on flanking elements of secondary structure in the fragment complex (Figure 1). At a 1:1 ratio of peptides (1 mM concentration) the isolated fragments and the complex are in slow exchange on the NMR time scale. We present a detailed thermodynamic analysis of the association process from pH- and temperature-dependent changes in the population of the folded state. The stability of native ubiquitin has been studied by similar methods to estimate the cost in free energy of the bimolecular association process and to estimate the extent to which nativelike interactions are established in the fragment complex. Studies of the isolated fragments, together with the work of others, suggest that the N-terminal fragment U(1−35) weakly populates nativelike β-hairpin and α-helical structure and that this fragment is a good candidate for nucleation of fragment condensation.

MATERIALS AND METHODS

Materials. Peptides were synthesized using standard Fmoc solid-phase chemistry (*32*) and purified by reverse-phase HPLC on a C8 column (Applied Biosystems Aquapore, 10 mm × 100 mm) with 0.1% trifluoroacetic acid and an acetonitrile gradient. Sample purity was checked by analytical HPLC and plasma desorption mass spectrometry and ^{1}H NMR spectroscopy. Peptide U(1−35) was synthesized as the C-terminal amide with a free N-terminus (mass 3904), U(36−76) as the *N*-acetyl derivative with a free C-terminus (mass 4719), and U(21−35) with both the N- and C-termini protected as *N*-acetyl and C-terminal amide, respectively (mass 1729). Bovine ubiquitin and ultrapure guanidine hydrochloride (Gdn·HCl) were purchased from Sigma and used without further purification. Gdn·HCl concentrations were determined by refractive index measurements (*33*).

NMR Methods. All NMR experiments were performed on a Bruker DRX500 spectrometer. Phase-sensitive double quantum filtered correlation spectroscopy (DQF-COSY; *34*), total correlation spectroscopy (TOCSY; *35*), nuclear Overhauser effect spectroscopy (NOESY; *36*) and rotating Overhauser effect spectroscopy (ROESY; *37*, *38*) experiments were performed by collecting 1−2K points in *f*2 and 400−600 points in *f*1. Quadrature detection in *f*1 was achieved by use of time-proportional phase incrementation (TPPI), and solvent suppression was achieved by presaturation or use of the WATERGATE solvent suppression sequence (*39*, *40*). TOCSY experiments employed a spin locking field of 5 kHz, and for ROESY experiments, 2 kHz. Data were processed on a Silicon Graphics Indy Workstation using Bruker XWINNMR software. Typically, a sine-squared window function shifted by $\pi/4-\pi/2$ was applied in both dimensions, with zero-filling in *f*1 to 1K points.

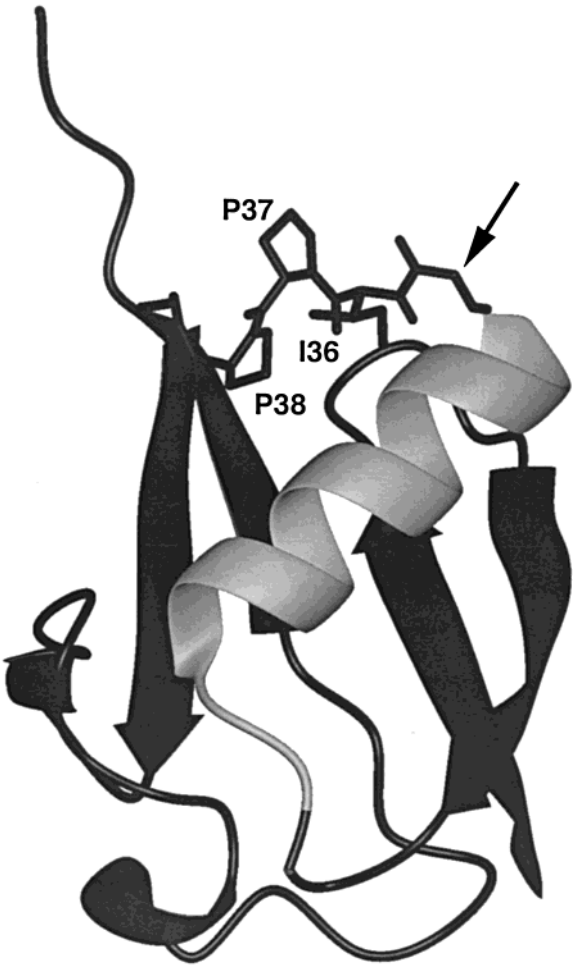

FIGURE 1: X-ray structure of bovine ubiquitin (PDB code 1ubq) illustrating the loop region adjacent to the helical sequence (residues 21−35). The arrow indicates the position of Gly35 at the end of the N-terminal peptide U(1−35) used for fragment complexation studies with U(36−76). Residues Ile36, Pro37, and Pro38 are also highlighted. Figure was drawn with MOLMOL (*42*).

Circular Dichroism Spectroscopy. CD spectra were acquired on an Aviv model 62DS spectrometer (Aviv Associates), with a 0.2 cm path length cell. Stock peptide solutions were prepared as 1 mg in 1 mL of solution. Samples were diluted with water, or aqueous methanol, to give 20 μM solutions for analysis by CD. Typically five scans were acquired over the wavelength range 190−250 nm in 1.0 nm steps with a bandwidth of 4 nm at 298 K. The resulting data were smoothed and baseline-corrected by solvent subtraction.

Thermodynamic Analysis. A two-state model was assumed in which the two peptide fragments associate cooperatively and reversibly (confirmed experimentally) to form a nativelike complex: U(1−35) + U(36−76) → U(1−35)·U(36−76). Equimolar concentrations of the two peptide fragments were combined such that the fraction of folded peptide f_F (estimated from the intensity of NMR signals) at a total concentration of each fragment c, gives an association constant K_{assn}, where

$$K_{assn} = f_F/[(1 - f_F)^2 c] \quad (1)$$

with $\Delta G°_{assn}$ calculated from $-RT \ln (K_{assn})$. $\Delta G°_{assn}$ shows a nonlinear temperature dependence enabling $\Delta H°_{assn}$, $\Delta S°_{assn}$, and $\Delta C_p°$ to be determined at 298 K by fitting the following expression to a nonlinear least-squares analysis with KaleidaGraph software (Synergy, Inc.):

$$\Delta G°_{assn} = [\Delta H°_{assn} + \Delta C_p° (T - 298)] - T[\Delta S°_{assn} + \Delta C_p° \ln (T/298)] \quad (2)$$

Values for $\Delta G°_{assn}$ were determined directly from integration of peak intensities in the NMR spectrum and are subject to relatively small uncertainties (≤5%). The resonances for Hϵ of His68 and Hϵ and Hδ of Tyr59 are clearly resolved for both the unfolded and folded states and were used to estimate populations. Similar populations were obtained in each case with no obvious distortions due to differential relaxation rates caused by differences in local dynamic behavior in the folded versus unfolded state. Errors in Table 1 for $\Delta H°_{assn}$, $\Delta S°_{assn}$, and $\Delta C_p°$ are fitting errors. Parameters were determined from a number of arbitrary starting values and all converged to the same final values (R >0.98). Various fixed values for $\Delta C_p°$ in the range ±50% of the value determined iteratively were also used; however, these all gave poorer fits to the data.

The folding of bovine ubiquitin was studied in various concentrations of denaturant (Gdn·HCl) and at various pHs. The population of the native folded state was monitored from the intensity of Hϵ of His68 close to the midpoint of the folding transition where the folded and unfolded states are in slow exchange on the NMR time scale. In this case, the Hδ and Hϵ of Tyr59 were obscured by the residual NH peak from the denaturant. The free energy of folding, $\Delta G°$, for the unimolecular process was calculated from the equilibrium constant $K = f_F/(1 - f_F)$. The protein stability in water ($\Delta G°_{water}$) was determined by the linear extrapolation method with the assumption

$$\Delta G° = \Delta G°_{water} - m[\text{Gdn·HCl}] \quad (3)$$

The thermodynamics of folding of ubiquitin at 298 K and at several pHs were determined from the temperature dependence of the population of the folded and unfolded states and the data were fitted to an expression similar to eq 2.

Molecular Modeling. Hydrophobic surface area burial, using a spherical probe of radius 1.4 Å, was calculated by the molecular modeling programs Macromodel (*41*) and MOLMOL (*42*) with the X-ray coordinates of ubiquitin (*26*) and random coil conformations generated in Macromodel.

RESULTS

Reconstitution of Complementary Fragments. The two peptide fragments U(1−35) and U(36−76) were mixed in equimolar proportions each at a concentration of 1 mM, and the degree of association monitored by ^{1}H NMR at 500 MHz using a number of well-resolved aromatic signals. The majority of resonances in the aromatic region of the spectrum arise from the C-terminal fragment; only Phe4 is present in the N-terminal part of the sequence. For example, Hϵ of His 68 at 8.63 ppm in the spectrum of U(36−76) alone splits into two signals of very similar intensity in the spectrum of the 1:1 mixture of fragments at pH 4.0. Similarly, the Hϵ and Hδ of Tyr59 are well-resolved into two equally populated species representing the folded and unfolded states (Figure 2). We see no evidence for other folded or partially folded states in equilibrium and estimate the stability of the complex by use of a simple two-state model (see Materials and Methods). The position of this equilibrium is sensitive to pH such that the fragments are more fully associated at high pH (Figure 3). On the basis of eq 1, $\Delta G°_{assn}$ is shown to have a linear dependence on pH, as illustrated in Figure 3.

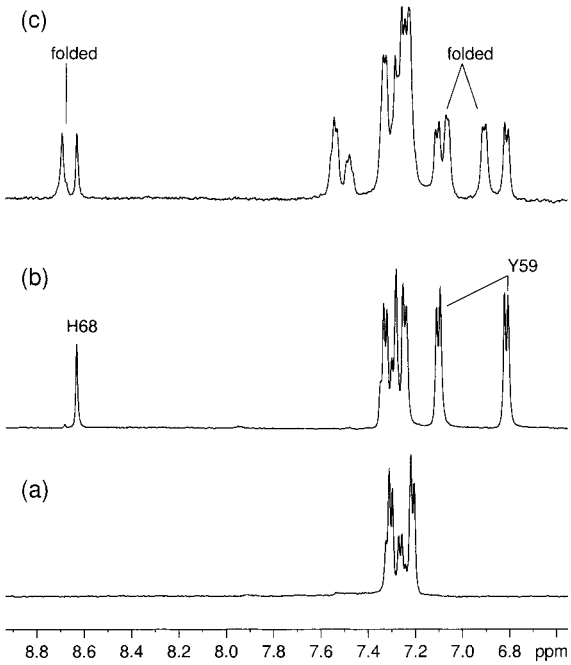

FIGURE 2: Portions of the aromatic region of the ^{1}H NMR spectra of the peptides U(1−35) (a), U(36−76) (b), and the 1:1 fragment complex at 298 K (c), all at pH 4.0 and peptide concentrations of 1 mM.

Which characteristics of the complex suggest a nativelike structure? The lowest downfield shifted Hα signal observed for native ubiquitin is that of Phe4 at 5.62 ppm. This signal is clearly evident at a very similar chemical shift in the fragment complex (Figure 4a), and >0.7 ppm downfield of that in the isolated N-terminal peptide. Similarly, the CδH$_3$ of Leu50 has a very large upfield ring current shift from Tyr59 and appears at −0.17 ppm in the native structure (Figure 4b); this signal is also visible at a very similar position in the spectrum of the fragment complex (Figure 4a) and gives a similar pattern of long-range NOEs, suggesting that this nativelike tertiary interaction is preserved. Similarly, the signals from His68 and Tyr59 (see above) have practically identical chemical shifts in the fragment complex and the native structure. Portions of the TOCSY spectrum showing the Hα−NH fingerprint regions of native ubiquitin, together with that of the complex, are shown in Figure 4c,d

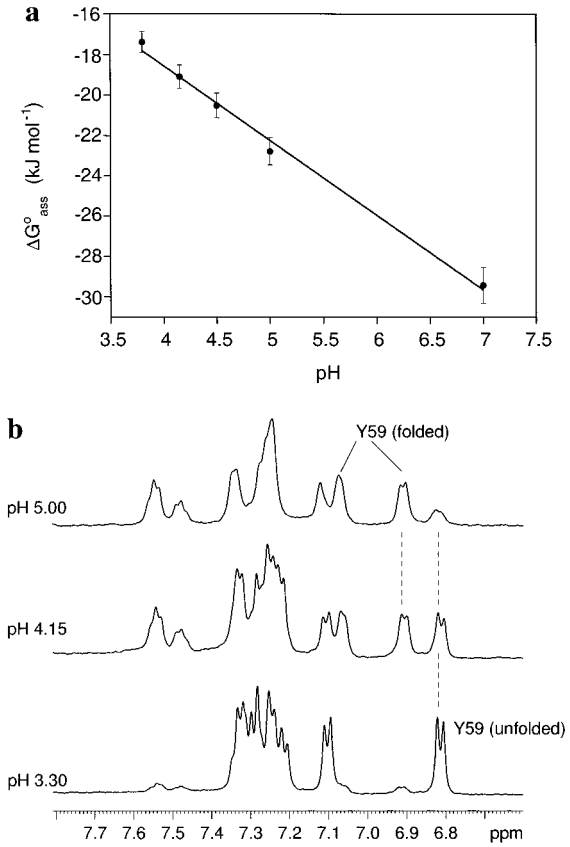

FIGURE 3: (a) pH dependence of the free energy of fragment association estimated from populations of the folded and unfolded states by ^{1}H NMR signal intensities at fragment concentrations of 1 mM at 298K (correlation coefficient $R > 0.98$). (b) Aromatic region of the ^{1}H NMR spectra of the 1:1 fragment complex at various pHs at 298 K showing changes in the population of the folded state; at pH 3.30, fragments are largely unfolded, and at pH 5.00, largely folded.

to illustrate the extent of the similarities of the two spectra. Data collection necessitated use of a relatively low pH to reduce NH exchange rates; under these conditions, and at this concentration, the two fragments are not fully associated, giving rise to residual cross-peaks in the TOCSY spectrum of the complex due to the unfolded fragments. However, there are clear similarities in the chemical shift dispersion observed for the fragment complex versus the native state (see below).

Thermodynamics of Fragment Association. Since resonances from both the unfolded peptide fragments and the complex are detected in the same spectrum, we are readily able to determine the change in the population of the folded state as a function of temperature. At 298 K and pH 4.0, we estimate $K_{assn} \approx 2 \times 10^3$ M^{-1} and $\Delta G^{\circ}_{assn} \approx -19$ kJ mol^{-1}. The change in ΔG°_{assn} with temperature is shown in Figure 5 and demonstrates a marked nonlinear relationship, with the stability maximum of the complex occurring around ~294 K. The pronounced curvature of this plot, with evidence for the on-set of cold denaturation, is consistent with ΔH°_{assn} and ΔS°_{assn} having a significant temperature dependence as a consequence of a large change in heat capacity for association of the fragments. Using eq 2, we have fitted the data to determine these parameters (Table 1). The data show that association of the fragments is enthalpy-driven at 298 K with a corresponding adverse entropy change. The latter is perhaps rather small given the bimolecular nature

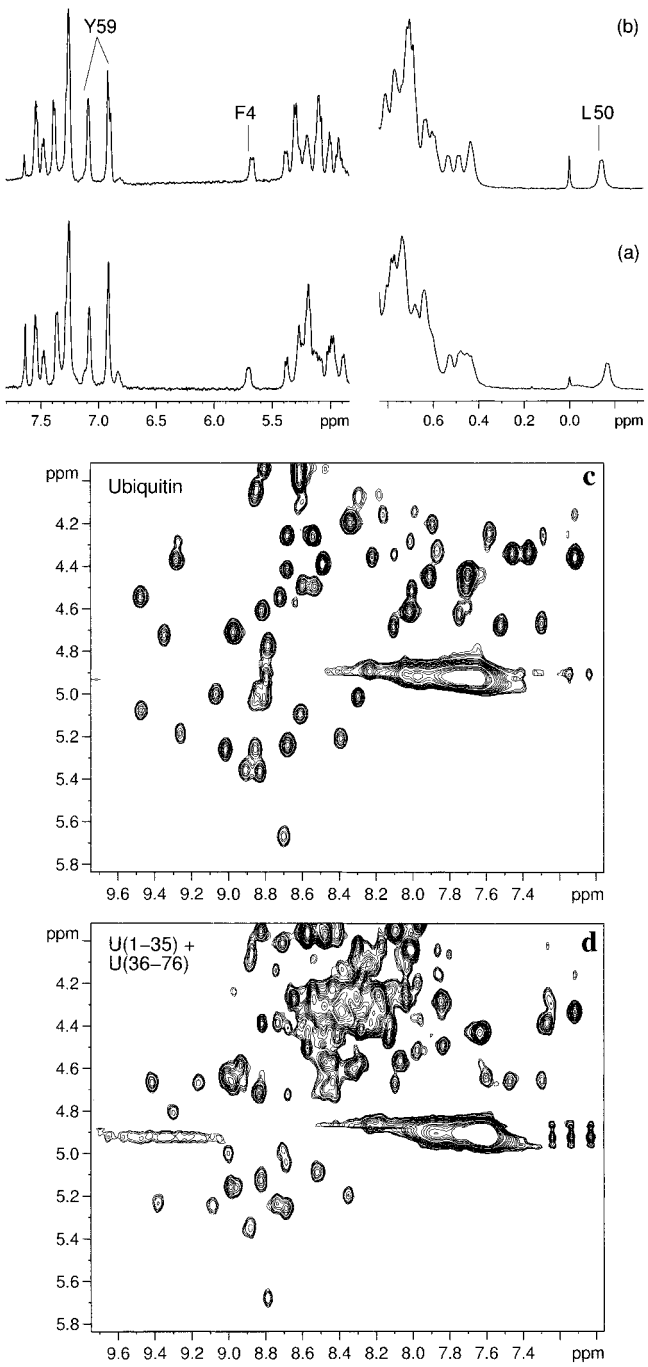

FIGURE 4: Comparison of portions of the 1D NMR spectra of the fragment complex (a) and native ubiquitin (b) at pH 7.0 and 298 K and of the NH to Hα fingerprint region of the TOCSY spectra of native ubiquitin (c) and the fragment complex [U(1−35) + U(36−76)] (d) recorded in 90% H_2O solution at 288 K and pH 4.0.

of the fragment association, although it is likely to be significantly offset by favorable entropic contributions from the hydrophobic effect. The data suggest that the complex is sufficiently well-ordered to bury a significant amount of hydrophobic surface area.

Thermodynamics of Folding of Native Ubiquitin. The stability of native ubiquitin has been investigated by guanidine hydrochloride denaturation experiments. NMR provides a convenient method of analysis because the folded and unfolded states are in slow exchange with each other on the NMR time scale at modest concentrations of denaturant and

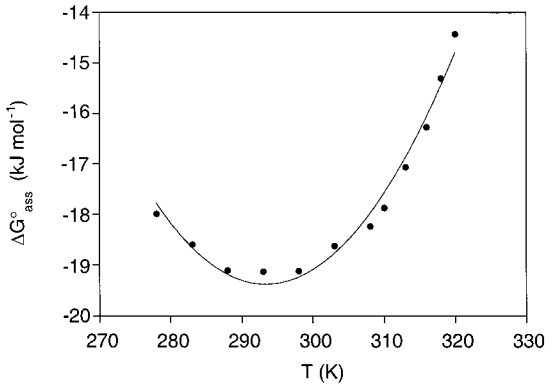

FIGURE 5: Temperature dependence of the free energy of association ($\Delta G°_{assn}$) of the peptide fragments U(1−35) and U(36−76) determined from the relative populations of the folded and unfolded states by ^{1}H NMR signal intensities (fragment concentrations of 1 mM at pH 4.0). The line of best fit to eq 2, from nonlinear regression analysis, is shown (correlation coefficient $R = 0.98$); thermodynamic parameters for folding are presented in Table 1.

low pH (*24*). The Hϵ of His68 is well-resolved and was used for monitoring the populations of the folded and unfolded states in the pH range 2.9−5.0 and over a range of concentrations of denaturant (0−7 M). A sigmoidal unfolding curve is observed in each case that is completely reversible upon dilution from high denaturant concentration, with the midpoint of the unfolding transition occurring around 3.5−4.0 M Gdn·HCl. The linear extrapolation method was used to estimate the stability of the folded state in water alone ($\Delta G°_{water}$) at pH 2.9, 3.9, and 5.0 (Figure 6) (*43*−*46*). The stability of native ubiquitin under denaturing conditions appears to be insensitive to pH in this range, within the experimental error of the measurement [$\Delta G°_{water} = -31$ ($\pm$1) kJ mol^{-1} at 298 K]. This contrasts with the stability of the fragment complex, which shows a significant increase in stability at higher pH. Similarly anomalous pH-dependent effects on stability in the presence of denaturants have recently been reported by Ibarra-Molero et al. (*19*) and are discussed in detail below.

A complete thermodynamic description of the folding−unfolding transition for ubiquitin has been determined in an analogous fashion to that described above by measuring the temperature dependence of the folded population in 4 M Gdn·HCl at pH 4.0 by NMR (Figure 7). Under these conditions both the folded and unfolded states are roughly equally populated at 298 K, as judged by a number of well-resolved NMR signals that are clearly split into two forms. Thus, although the relative stability of the folded and unfolded conformations are similar ($\Delta G° \approx 0$), the NMR data show that the two states are in slow exchange, indicating a large kinetic barrier that ensures the cooperative integrity and specificity of the folded state. The protein shows a clear stability maximum ($\Delta S° = 0$) at 300 K, with denaturation occurring both above and below this temperature, in agreement with previous studies that indicate that ubiquitin undergoes cold denaturation (*18, 19*). Folding is endothermic in the presence of Gdn·HCl denaturant and is associated with a large change in heat capacity, as estimated from the fit to the experimental data with eq 2. Calculated parameters are shown in Table 1.

Cost of a Bimolecular Association. One method of assessing the stability of the native structure arising from covalent attachment of the two fragments is to use "effective molarity" as a measure of entropic cooperativity (*47*). The effective molarity K_{eff} represents the ratio of equilibrium constants for the unimolecular (K_{uni}) and bimolecular association (K_{assn}) processes ($K_{eff} = K_{uni}/K_{assn}$). We have compared the K_{assn} values for fragment complexation shown in Figure 3 with the K_{uni} values for native ubiquitin derived calorimetrically from the DSC measurements of Ibarra-Molero et al. (*19*). The latter were estimated over a relatively small pH range of 2−4 because of the high thermal stability of ubiquitin close to physiological pH. In contrast, our data were collected in the range 3.8−7.0; below pH 3.8 complex formation is more difficult to quantitate. The linear relationship that we observe between complex stability and pH has enabled us to extrapolate the data to pH 3.0. The very different slope of the stability−pH plot for fragment complexation, compared with the native structure, results in a very strong pH dependence of K_{eff}, which is small at pH 3.0 ($K_{eff} \approx 5$ M), indicating only marginally different stabilities, rising to $K_{eff} \approx 100$ M at pH 4.0, all at 298 K. A similar analysis of the folding of fragments of the B1 domain of protein G yields a K_{eff} value of $\approx$6 M at pH 5.9 and 298 K, although pH-dependent effects were not investigated (*14*).

We have also calculated K_{eff} values using data derived from the linear extrapolation method. Here we see very little pH dependence of ubiquitin stability, as already discussed. As a result K_{eff} is smaller at pH 4.0, $\approx$200 M versus $\approx$600 M at pH 3.0, 298 K. Even over this limited pH range, these are surprisingly small numbers given that much larger values (10^2−10^9 M) are measured experimentally for covalent bond formation in a variety of inter- versus intramolecular reactions of small organic molecules (*48*). One possible explanation for the small values of K_{eff} is that "fraying" of the free ends of the polypeptide chain at the cleavage site, compared with the highly restricted backbone in the native protein structure, may significantly offset the entropic cost of the bimolecular association (see below). In the present study, consecutive proline residues (Pro37 and Pro38) are found immediately adjacent to the cleavage site (Figure 1). It is conceivable that the absence of strain at this junction in the complex of the two fragments could partially offset the cost of the bimolecular association.

Several other groups have assessed the stability of fragment complexes of a number of other small proteins of comparable size to ubiquitin. Stabilities generally seem to be larger than reported in this work ($K_{assn} = 2.6 \times 10^4$ M^{-1} at pH 6.0), although there is some variability of the conditions under which the studies were conducted. Chymotrypsin inhibitor 2 (CI-2) has a K_{assn} value estimated to be (1−2.5) $\times 10^7$ M^{-1} at pH 6.3 (*13*), while a fragment complex of the B1 domain of protein G has $K_{assn} \approx 1 \times 10^5$ M^{-1} at pH 5.5 (*14*), and barnase has $K_{assn} \approx 1.7 \times 10^6$ M^{-1} (*11*), all of which are more stable than the ubiquitin complex.

Nucleation Sites for Folding: Conformational Analysis of the Isolated Fragments. The U(1−35) N-terminal peptide, and several truncated analogues, have been studied in solution by NMR (*30*). A high degree of nativelike structure has been reported in 60% aqueous methanol, in which the β-hairpin (residues 1−17) and α-helical portions (residues 21−34) of the sequence are significantly populated. More recently, the β-hairpin peptide has been examined in detail in purely aqueous solution where there is good evidence from

Table 1: Thermodynamic Parameters ($\Delta H°$, $\Delta S°$, and $\Delta C_p°$ at 298 K and Extrapolated to 333 K) for Fragment Complexation and Ubiquitin Folding

	$\Delta H°$ (kJ mol^{-1})	$\Delta S°$ (J K^{-1} mol^{-1})	$\Delta C_p°$ (J K^{-1} mol^{-1})
U(1−35) + U(36−76), NMR at 298 K	−37.5 (±1.6)	−61.3 (±5.4)	−3904 (±280)
U(1−35) + U(36−76), NMR extrapolated to 333 K	−174 (±10)	−494 (±35)	−3904 (±280)
native ubiquitin, NMR at 298 K	+9.8 (±1.5)	+31.3 (±5.3)	−5180 (±244)
native ubiquitin, NMR extrapolated to 333 K	−171 (±9)	−544 (±26)	−5180 (±244)
native ubiquitin, DSC at 333 K[a]	−208	−561	−3760

[a] DSC data from Wintrode et al. (*20*); errors not given.

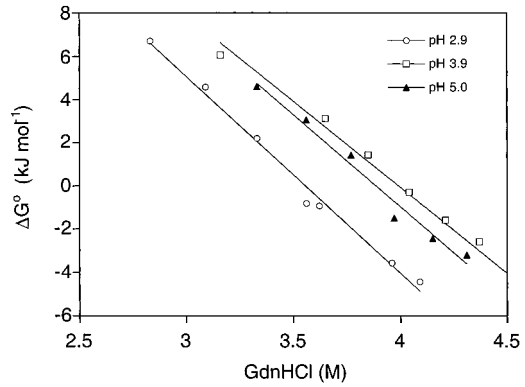

FIGURE 6: Linear extrapolation plots for native ubiquitin showing the free energy of folding at 298 K as a function of Gdn·HCl concentration at pH 2.9 (○), 3.9 (□) and 5.0 (▲) (in all cases correlation coefficient $R > 0.98$); populations of the folded and unfolded states, which are in slow exchange on the NMR time scale, were measured from the ^{1}H NMR signal intensity of the Hϵ of His68 for 1 mM samples of ubiquitin

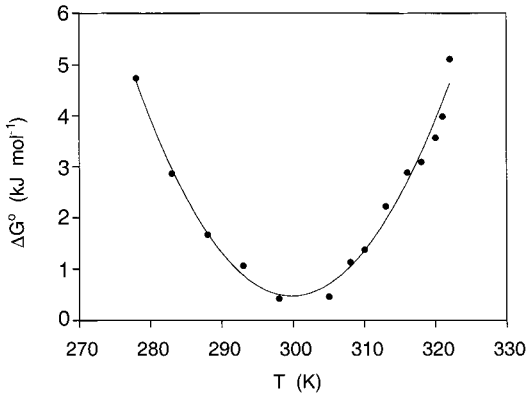

FIGURE 7: Temperature-dependent stability of native ubiquitin (1 mM concentration, pH 4.0 in 4.0 M Gdn·HCl) determined from the relative populations of the folded and unfolded states estimated from ^{1}H NMR signal intensities. The line of best fit is that from nonlinear regression analysis (correlation coefficient $R > 0.98$); thermodynamic parameters for folding are presented in Table 1.

NOE data for a small population of nativelike structure (*31*). Our own results are consistent with these findings (unpublished data).

In addition, we have investigated the isolated α-helical peptide (residues 21−35) for evidence of autonomous folding in water. The core residues of the helix, namely contiguous residues from V26 through to I30, show small upfield deviations of Hα shifts from random coil values of ≈0.1 ppm, and deviations of $^3J_{NH-H\alpha}$ values in the range 0.4−0.9 Hz, suggesting the presence of some nascent helical structure. Upon addition of methanol or trifluoroethanol, the peptide is observed by far-UV CD to undergo a cooperative transition to the folded state with a high proportion of helix present above 30% trifluoroethanol (data not shown). Much larger

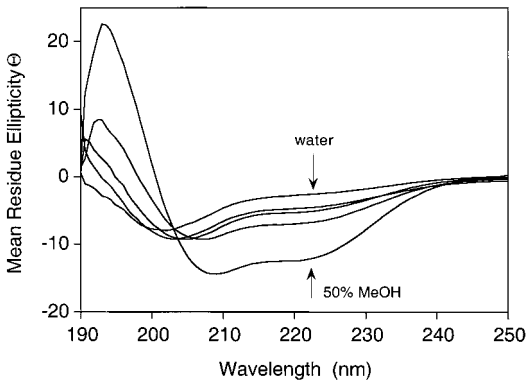

FIGURE 8: Far-UV CD spectra of peptide U(36−76) recorded at 293 K as a function of aqueous methanol concentration (0−50% v/v); mean residue ellipticity θ is expressed in degrees times square centimeters per decimole × 10^{-3}.

deviations of Hα shifts of between 0.2 and 0.4 ppm for I23 through to Q31, and deviations of $^3J_{NH-H\alpha}$ values > 2 Hz, support this conclusion. We have calculated a family of structures for the α-helical sequence from NOE data collected in 40% aqueous TFE solution. We see a large number of *i*, *i* + *3* NH to Hα NOEs and side-chain−side-chain interactions consistent with core helical structure. However, the C-terminal five residues are relatively disordered, showing few characteristic α-helical NOEs even under the helix-forcing conditions employed. Using the linear extrapolation method and assuming a two-state model for folding of the N-terminal residues of the helix (*11*, *49*), we have fitted the sigmoidal solvent-induced folding curve observed by CD (θ_{222}) and estimate the stability of the helix in water at 298 K to be ≈+9 kJ mol^{-1} (folded population of ≈3%). Structure prediction with AGADIR (*50*) similarly indicated a very low population of folded helix in water over a range of pHs.

The C-terminal peptide U(36−76) has also been investigated by CD and NMR for evidence of residual structure in aqueous solution. The CD spectrum of U(36−76) shows a negative absorption at ∼200 nm, indicative of largely random coil conformation (Figure 8). However, titration with methanol results in an increase in negative ellipticity at 208 and 222 nm and increasingly positive ellipticity at 194 nm. These features are consistent with a structural transition to an ensemble of highly populated α-helical conformations in the presence of the organic cosolvent. Similarly, the methanol denatured state of native ubiquitin also shows a high propensity to adopt nonnative secondary structure, as also reported by others (*51*−*53*). The chemical shift dispersion of U(36−76) is sufficiently poor in aqueous solution that complete and specific assignment of all backbone NH and Hα resonances was difficult to obtain. Narrow line widths are indicative of rapid conformational averaging about backbone ϕ and ψ angles. The seven Leu residues of U(36−

76), which occur largely in β-sheet within the C-terminal half of native ubiquitin, have Hα chemical shifts in the range 4.07−4.35 ppm indicating upfield deviations of up to ≈0.3 ppm from random coil values (*54*−*56*). Thus, even in aqueous solution there is the suggestion that some residue backbone torsion angles are sampling nonnative α-helical conformational space.

Previous studies have shown that methanol is a less potent α-helix-inducing solvent than trifluoroethanol (TFE), frequently promoting nativelike secondary structure formation without the nonspecific solvation effects that are associated with the helix-forcing tendencies of TFE (*57*−*59*). In a peptide derived from the N-terminus of ferredoxin, we showed that methanol cosolvent only promoted formation of a nativelike β-hairpin, while TFE at low concentrations produced a complex equilibrium involving both sheet and nonnative helical structure. It is noteworthy that in the methanol titration with U(36−76) the equilibrium is readily displaced from random coil to α-helical structure, despite the β-sheet propensity of many of the residues in this peptide fragment in native ubiquitin. Cox et al. (*30*) showed that the accuracy of secondary structure prediction calculations on ubiquitin is much higher in the N-terminal portion of the sequence (residues 1−35) than in the C-terminus (residues 36−76) and that secondary structure in the C-terminal segment would appear to be largely imposed by tertiary interactions from residues in remote parts of the sequence. The observed effects of the methanol titration in inducing α-helical structure we attribute to nonspecific solvation effects in a sequence that has a low intrinsic nativelike structural propensity.

DISCUSSION

pH-Dependent Stability of the Fragment Complex and Native Ubiquitin. Using the linear extrapolation method (*33*, *43*−*46*), we have estimated the stability of native ubiquitin in water at a number of different pHs. The stability is largely insensitive to pH over the range 2.9−5.0 in the presence of denaturant. In contrast, association of the peptide fragments, which we assess in water alone from the population of the folded and unfolded states, shows a significant pH dependence (Figure 3). Since polar side chains are largely solvent-exposed on the protein surface and ionic interactions are likely to contribute to protein stability through salt bridges, changes in pH are expected to change the ionization states of some residues (particularly carboxylate groups over the low pH range studied), resulting in disruption of these charge−charge interactions and a reduction in overall stability (*23*, *60*−*63*). Recent studies using both the linear extrapolation method from high guanidine hydrochloride concentration, in parallel with calorimetry methods in pure water, have highlighted a similar discrepancy in the effects of denaturants on pH-dependent stabilities (*19*). One explanation is that the effect of high concentrations of protein denaturant is to "screen" ionic interactions between side chains (*23*, *64*), as recently demonstrated for ionic interactions between helices in myoglobin (*65*). Guanidine hydrochloride is likely to be particularly effective in binding to surface exposed charged groups either through the guanidinium cation or chloride anion such that the overall contribution to protein stability of surface salt bridges is likely to be small and, as a consequence, relatively pH-insensitive. It is noteworthy that other proteins do show significant pH-dependent stabilities determined from guanidine-induced denaturation curves (*66*, *67*), suggesting that some charge−charge interactions on the surface of proteins do benefit from partial surface burial and reduced access to solvent and denaturants. The slope (m) of the linear extrapolation plot of $\Delta G°$ as a function of [Gdn·HCl] also appears to be invariant with pH, within experimental error (Figure 6). This observation suggests that changes in the solvent-accessible surface area between the folded and unfolded states varies little as a function of pH, although other studies have identified pH-dependent effects, which have been interpreted in terms of an "expansion" of the unfolded state through electrostatic repulsions of positive charges at low pH (*66*). It seems highly likely that the pH invariance of $\Delta G°$ and m values for ubiquitin derived from the linear extrapolation method find a common origin in the screening effects of denaturant strongly masking the effects of pH on specific charge−charge interactions (*19*).

The slope of $\Delta G°_{assn}$ versus pH for fragment complexation, and $\Delta G°$ versus pH for folding of native ubiquitin, should give some indication of the extent to which surface-exposed ionic interactions contribute to the overall stability of the two structures in the absence of the denaturant (*68*). In Figure 3, we plot the pH-dependent stability profile of the fragment complex, which gives a slope $m_{pH} = -3.7$ kJ mol^{-1} per unit of pH. In contrast the data for native ubiquitin derived from the calorimetry data of Ibarra-Molero et al. (*19*), also in the absence of denaturant, has a significantly larger value of $m_{pH} \approx -15$ kJ mol^{-1} per unit of pH over the linear portion of their plot (pH 2.5−3.5). Ibarra-Molero et al. (*19*) similarly investigated the pH-dependent stability profile of yeast ubiquitin that differs from the bovine protein in three conservative substitutions (P19S, E24D, and A28S, all in the N-terminal helix and preceding loop region) but has essentially the same structure (*69*). Despite these small sequence differences, the stability is markedly reduced ($\Delta G° \approx -22$ kJ mol^{-1} versus -30 kJ mol^{-1} at pH 4), with the yeast protein showing a less pronounced pH-dependent stability profile with slope m_{pH} of ≈−10 kJ mol^{-1} per unit of pH (over the pH range 2−4). This is despite the fact that there is no difference in the nature and number of ionizable groups between the two proteins. As our data show, further destabilization of the structure through fragmentation results in a further reduction in m_{pH}. One possible explanation for the lower sensitivity to pH of the fragment complex is that the structure is less compact and considerably more dynamic ("molten globule-like") in nature, such that surface interactions have an intrinsically smaller contribution to the stability of the complex than in the native state. The difference between the bovine and yeast structures is less obvious since X-ray analysis shows them to have similar compact folds (*69*). Alternatively, there could be differences in solvent accessibility in the unfolded states that are more difficult to assess (*70*). Shortle and Meeker (*67*) have shown that point mutations do affect apparent m values for staphylococcal nuclease mutants, which they attribute to changes in the denatured ensemble, although deviations from a two-state unfolding model have been suggested as an alternative (*65*).

Evidence for a Compact Nativelike Complex of the Peptide Fragments. The possibility of a molten globule state for the fragment complex has been examined by comparing the

chemical shift perturbations of Hα resonances from random coil values with those for the native protein under similar conditions. As has previously been argued (*10, 71*), the magnitude of downfield shifts of Hα resonances in protein β-sheets is, in large part, a consequence of the anisotropic effects of carbonyl groups on the opposing strand. The magnitude of Hα shifts should, therefore, be correlated with mean hydrogen-bonding distance or "compactness" of the folded state (*72*). Hα chemical shifts in the complex show all the hallmarks of a compact cooperatively folded structure (*54, 55*). A number of buried methyl groups have substantial ring current shifts in the native structure (see Figure 4) and show analogous shifts in the fragment complex, suggesting a similar highly organized hydrophobic core. Although the stability of the fragment complex changes significantly with pH, it is noticeable that the chemical shifts of the folded state are largely insensitive to pH, confirming that only the overall stability, but not the cooperative integrity of the nativelike folded structure, changes with pH. Many β-sheet NH and Hα resonances of the fragment complex are well-resolved in the TOCSY spectrum in H_2O (Figure 4), showing similarity with the native protein, consistent with the β-sheet core of the fragment complex retaining a similar hydrogen-bonded network as the native state. It is evident from the TOCSY data in Figure 4 that although many cross-peaks in the fingerprint region have similar shifts, the spectra are not identical. Focusing on clearly resolved downfield-shifted Hα resonances that belong to residues that lie in β-sheet (δHα $>$ 4.8 ppm) reveals differences of typically 0−0.2 ppm that suggest some minor structural rearrangement or repacking of side chains, in agreement with other fragment complexation studies (*12, 13*). These are not necessarily a consequence of a "loosening" of the structure because a number of Hα resonances appear to be further downfield in the β-sheet of the fragment complex, rather than shifted back toward the random coil values.

The α-helical residues are less readily identified on account of overlap with signals from the uncomplexed fragments U(1−35) and U(36−76), which are also present in the TOCSY fingerprint region. However, in studies of the isolated α-helical fragment U(21−35) in strongly helix-inducing TFE solution, the C-terminal five residues are quite disordered, suggesting that significant helix fraying in the fragment complex is also a possibility. The latter observation perhaps offers an explanation for the relatively small value of K_{eff} (ratio of stability constants for the unimolecular versus bimolecular folding process). On one hand, the fraying of the "loose ends" of both the N- and C-terminal fragments may help to lower the entropic cost of the bimolecular association, while the same part of the peptide backbone in the native structure will be more rigidly constrained. Of course, some small loss of hydrophobic surface burial between helix and sheet, as a consequence of end fraying, may also need to be factored into the equation. On the other hand, some global structural optimization through relief of strain energy may also be beneficial to fragment complexation. Overall, the fragment complex retains a largely nativelike compact fold, folding and unfolding in a highly cooperative fashion in response to changes in temperature and pH.

Thermodynamics of Folding: Fragment Complexation versus Native Structure. The temperature dependence of the population of the folded state in equilibrium with the unfolded form has proved a powerful method for determining the thermodynamics of folding of both the fragment complex and native ubiquitin by NMR. The data (presented in Table 1) have been determined at 298 K and are therefore most accurate at this temperature. Our estimate of ΔC_p° for folding of native ubiquitin of -5.2 (± 0.3) kJ mol^{-1} K^{-1} compares favorably with extrapolated calorimetric estimates of ΔC_p° at 298K from Woolfson et al. (*21*) of -4.8 (± 0.5) kJ mol^{-1} K^{-1}, Wintrode et al. (*20*) of -5.7 kJ mol^{-1} K^{-1}, and Ibarra-Molero et al. (*19*) of -3.76 (± 0.8) kJ mol^{-1} K^{-1}, the latter from analogous studies in Gdn·HCl, where cold denaturation is also observed by differential scanning calorimetry (DSC) analysis. By comparison, the change in heat capacity for fragment association at 298 K, estimated from the data in Figure 5, gives a value of -3.9 (± 0.3) kJ mol^{-1} K^{-1}, in reasonable agreement with the above data, given the relatively large uncertainties in some of these parameters. The data suggest that association of the fragments leads to similar changes in buried surface area, in support of the structural similarities already highlighted.

In many cases, good agreement has been reported between thermodynamic parameters for folding derived from thermal (DSC) and chemical denaturation methods (*66, 73*). When we compare ΔH° and ΔS° for fragment complexation versus folding of native ubiquitin we see some differences. While fragment complexation at 298 K is enthalpy-driven and has an adverse entropy term (Table 1), the data for native ubiquitin derived from Figure 5 show folding to be marginally entropy-driven with a small adverse enthalpy term. To permit comparisons between different data sets for different proteins, Robertson and Murphy (*73*) have extrapolated ΔH° and ΔS° to a common temperature (333 K) using experimental values for ΔC_p°. Data from DSC measurements on native ubiquitin at a T_m of 333 K give ΔH°_{333} of -208 kJ mol^{-1} and ΔS°_{333} of -561 J K^{-1} mol^{-1}. Extrapolation from our NMR denaturation data to 333 K shows reasonable agreement ($\Delta H^\circ_{333} = -172$ kJ mol^{-1} and $\Delta S^\circ_{333} = -544$ J K^{-1} mol^{-1}), indicating that these parameters are reproducible by different methods (*66*). Extrapolation of the data for fragment complexation to 333 K ($\Delta H^\circ_{333} = -174$ kJ mol^{-1} and $\Delta S^\circ_{333} = -494$ J K^{-1} mol^{-1}) also shows consistency with the data for the native protein. The similarities in ΔH° for the unimolecular versus bimolecular process suggest that nativelike electrostatic and van der Waals interactions in the fragment complex are firmly established. Given the uncertainties in ΔC_p° measurements and the fact that our parameters are measured at 298 K, these similarities must be considered in the context of potentially large extrapolation errors.

Mechanism for Ubiquitin Folding and Implications for Fragment Association. Early hydrogen-bonding events in the folding of bovine ubiquitin have been investigated by hydrogen−deuterium exchange labeling in conjunction with rapid mixing techniques. Amide protons in the β-sheet and α-helix, as well as protons at the sheet/helix interface, have been shown to be protected in an initial 8 ms folding phase (*24*), indicating that these two elements of structure form in a common cooperative folding event. Gladwin and Evans (*25*) have shown, on an even faster time scale, that any secondary structure formation must occur only marginally ahead of a major cooperative event. The observation of

residual nativelike structure in the isolated N-terminal β-hairpin (1−17) (*31*), and a very low population of nascent α-helical conformation in fragment 21−35, as described here, is consistent with these marginally populated elements of structure acting as folding nucleation sites. The close proximity of these two elements of structure within the N-terminal half of the sequence, both of which are encompassed within peptide U(1−35), suggests the possibility that the mechanism of fragment complexation may also be a consequence of this half of the protein sequence acting as a nucleating template around which the two fragments are able to fold. On entropic grounds, β-hairpin and α-helix coalescence within U(1−35) requires the loss of a minimum amount of conformational entropy to bring these two elements of structure into close proximity, with partial formation of the hydrophobic core.

Surface area burial within the folded N- and C-terminal fragments, and at the interface between the associated fragments, has been modeled with the X-ray coordinates of the native folded structure (*26*), and random coil conformations generated for fragments 1−35 and 36−76 and for unfolded native ubiquitin with molecular dynamics simulations and energy minimization. Roughly similar proportions of nonpolar surface area are buried in the folding of the isolated fragments 1−35 and 36−76 and at the interface between the two folded components. These are 31%, 33%, and 36%, respectively, of the total surface area buried in the folding of native ubiquitin. In the case of the N-terminal fragment, hydrophobic burial involves largely elements of regular secondary structure, but in the C-terminal fragment core hydrophobic interactions are formed by less regular elements of structure (flexible loop regions) that are brought together by the overall folded topology (Figure 1). Association of the two fragments leads to the consolidation of the hydrophobic core of the protein. Analysis of intra- and interfragment hydrophobic surface area burial suggests that a major cooperative folding event for fragment complexation, analogous to that described by Gladwin and Evans (*25*) for the folding of native ubiquitin, could involve simultaneous hydrophobic burial within each partially folded fragment and at the fragment interface.

Recently, Plaxco et al. (*74*) introduced the term "relative contact order" to quantify the overall complexity of a protein fold. This parameter provides a measure of the average distance in sequence between interacting residues, normalized with respect to the chain length. Their data showed that there is a good correlation between the folding rate and contact order, with low values of the latter being associated with faster folding. Chiti et al. (*75*) have shown that different proteins with similar topologies but different contact orders, as a result of different loop sizes or lengths of elements of secondary structure, show different folding rates, in support of this model. The implication of these results is that any transition state must gain enough structure for further conversion to the native state to occur rapidly. This implies that nucleation events would benefit from a few stabilizing interactions between portions of the polypeptide chain for which there is a small entropic penalty for bringing these regions together (*76*). Thus, "partial" contact orders within regions of the polypeptide chain may provide some insight into possible nucleation sites for folding.

Examining the complexation of ubiquitin fragments within this framework suggests that the N-terminal portion of the sequence provides the most likely nucleation site around which fragment complexation can take place. Calculation of contact orders (COs) for native ubiquitin (0.151) and partial contact orders for the two fragments [0.124 for U(1−35) and 0.172 for U(36−76)] (K. Plaxco, personal communication) is consistent with this suggestion, with the U(1−35) fragment having the lowest partial CO value. The evidence from studies of the smaller peptide fragments U(1−17) (*31*), and to a much lesser extent U(21−35), that low levels of nativelike structure persist adds further weight to this conclusion. Protein engineering methods, coupled with detailed kinetic analysis, have suggested that residues in the N-terminal half of the sequence are involved in a productive intermediate that is populated at an early stage in the folding process (*77*). In the case of the C-terminal peptide fragment, NMR evidence in water from chemical shift data, together with the solvent-induced effects seen in aqueous methanol by CD, show that U(36−76) readily adopts nonnative α-helical structure. These data demonstrate a very low intrinsic nativelike structural propensity for fragment U(36−76) that must be imposed by tertiary interactions in the native state.

ACKNOWLEDGMENTS

We are grateful to Dr. Kevin Plaxco for a preprint of some recent results, for calculating partial contact orders for the ubiquitin fragments, and for helpful discussions on this subject. We also thank Guy Hill for collecting some preliminary data on the helical peptide U(21−35).

REFERENCES

1. Kim, P. S., and Baldwin, R. L. (1982) *Annu. Rev. Biochem. 51*, 459−489.
2. Dill, K. A. (1990) *Biochemistry 29*, 7133−7155.
3. Itzhaki, L. S., Otzen, D. E., and Fersht, A. R. (1995) *J. Mol. Biol. 254*, 260−288.
4. Baldwin, R. L., and Rose, G. D. (1999) *Trends Biochem. Sci. 24*, 26−33.
5. Baldwin, R. L., and Rose, G. D. (1999) *Trends Biochem. Sci. 24*, 77−83.
6. Baldwin, R. L. (1995) *Biophys. Chem. 55*, 127−135.
7. Munoz, V., and Serrano, L. (1995) *J. Mol. Biol. 245*, 275−296.
8. Stapley, B. J., and Doig, A. J. (1997) *J. Mol. Biol. 272*, 465−473.
9. Gellman, S. H. (1998) *Curr. Opin. Chem. Biol. 2*, 717−725.
10. Griffiths-Jones, S. R., Maynard, A. J., and Searle, M. S. (1999) *J. Mol. Biol. 292*, 1051−1069.
11. Sancho, J., and Fersht, A. R. (1992) *J. Mol. Biol. 224*, 741−747.
12. Kobayashi, N., Honda, S., Yoshii, H., Uedaira, H., and Munekata, E. (1995) *FEBS Lett. 366*, 99−103.
13. De Prat Gay, G., and Fersht, A. R. (1994) *Biochemistry 33*, 7957−7963.
14. Honda, S., Kobayashi, N., Munekata, E., and Uedaira, H. (1999) *Biochemistry 38*, 1203−1213.
15. De Prat Gay, G. (1996) *Protein Eng. 9*, 843−847.
16. Dill, K. A., and Shortle, D. (1991) *Annu. Rev. Biochem. 60*, 795−825.
17. Wright, P. E., Dyson, H. J., and Lerner, R. A. (1988) *Biochemistry 27*, 7167−7175.
18. Ibarra-Molero, B., Makhatadze, G. I., and Sanchez-Ruiz, J. M. (1999) *Biochim. Biophys. Acta 1429*, 384−390.
19. Ibarra-Molero, B., Loladze, V. V., Makhatadze, G. I., and Sanchez-Ruiz, J. M. (1999) *Biochemistry 38*, 8138−8149.

20. Wintrode, P. L., Makhatadze, G. I., and Privalov, P. L. (1994) *Proteins*: *Struct., Funct., Genet. 18*, 246−253.
21. Woolfson, D. N., Cooper, A., Harding, M. M., Williams, D. H., and Evans, P. A. (1993) *J. Mol. Biol. 229*, 502−511.
22. Khorasanizadeh, S., Peters, I. D., Butt, T. R., and Roder, H. (1993) *Biochemistry 32*, 7054−7063.
23. Makhatadze, G. I., Lopez, M. M., Richardson, J. M., and Thomas, S. T. (1998) *Protein Sci. 7*, 689−697.
24. Briggs, M. S., and Roder, H. (1992) *Proc. Natl. Acad. Sci. U.S.A. 89*, 2017−2021.
25. Gladwin, S. T., and Evans, P. A (1996) *Folding Des. 1*, 407−417.
26. Vijay-Kumar, S., Bugg, C. E., and Cook, W. J. (1987) *J. Mol. Biol. 194*, 531−544.
27. Weber, P. L., Brown, S. C., and Mueller, L. (1987) *Biochemistry 26*, 7282−7290.
28. Di Stefano, D. L., and Wand, A. J. (1987) *Biochemistry 26*, 7272−7281.
29. Harding, M. M., Williams, D. H., and Woolfson, D. N. (1991) *Biochemistry 30*, 3120−3128.
30. Cox, J. P. L., Evans, P. A., Packman, L. C., Williams, D. H., and Woolfson, D. N. (1993) *J. Mol. Biol. 234*, 483−492.
31. Zerella, R., Evans, P. A., Ionides, J. M. C., Packman, L. C., Trotter, B. W., Mackay, J. P., and Williams, D. H. (1999) *Protein Sci. 8*, 1320−1331.
32. Bodanszky, M., and Bodanszky, A. (1994) *The Practice of Peptide Synthesis*, 2nd ed., Springer-Verlag, Berlin.
33. Pace, C. N., and Scholtz, J. M. (1997) *Protein Structure − A practical approach* (Creighton, T. E., Ed.). 2nd ed. IRL Press, New York.
34. Piantini, U., Sorensen, O. W., and Ernst, R. R. (1982) *J. Am. Chem. Soc. 104*, 6800−6801.
35. Braunschweiler, L., and Ernst, R. R. (1983) *J. Magn. Reson. 53*, 521−528.
36. Jeener, J., Meier, B. H., Bachmann, P., and Ernst, R. R. (1979) *J. Phys. Chem. 71*, 4546−4553.
37. Bax, A., and Davis, D. G. (1985) *J. Magn. Reson. 63*, 207−213.
38. Bothner-by, A. A., Stephens, R. L., Lee, J., Warren, C. D., and Jeanloz, R. W. (1984) *J. Am. Chem. Soc. 106*, 811−812.
39. Piotto, M., Saudek, V., and Sklenar, V. (1992) *J. Biomol. NMR 2*, 661−665.
40. Sklenar, V., Piotto, M., Leppik, R., and Saudek, V. (1993) *J. Magn. Reson. A 102*, 241−245.
41. Mohammadi, F., Richards, N. G. J., Guida, W. C., Liskamp, R., Lipton, M., Caufield, C., Chang, G., Hendrickson, T., and Still, W. C. (1990) *J. Comput. Chem. 11*, 440−451.
42. Koradi, R., Billeter, M., and Wuthrich, K. (1996) *J. Mol. Graph. 14*, 51−55.
43. Pace, C. N. (1986) *Methods Enzymol. 131*, 266−280.
44. Bolen, D. W., and Santoro, M. M. (1988) *Biochemistry 27*, 8069−8074.
45. Santoro, M. M., and Bolen, D. W. (1988) *Biochemistry 27*, 8063−8068.
46. Santoro, M. M., and Bolen, D. W. (1992) *Biochemistry 31*, 4901−4907.
47. Creighton, T. E. (1993) *Proteins: Structures and Molecular Properties*, 2nd ed., W. H. Freeman and Co., New York.
48. Page, M. I., and Jencks, W. P. (1971) *Proc. Natl. Acad. Sci. U.S.A. 68*, 1678−1683.
49. Bolin, K. A., Pitkeathly, M., Miranker, A., Smith, L. J., and Dobson, C. M. (1996) *J. Mol. Biol. 261*, 443−453.
50. Lacroix, E., Viguera, A. R., and Serrano, L. (1998) *J. Mol. Biol. 284*, 173−191.
51. Wilkinson, K. D., and Mayer, A. N. (1986) *Arch. Biochem. Biophys. 250*, 390−399.
52. Stockman, B. J., Euvrard, A., and Scahill, T. A. (1993) *J. Biomol. NMR 3*, 285−296.
53. Brutscher, B., Bruschweiler, R., and Ernst, R. R. (1997) *Biochemistry 36*, 13043−13053.
54. Wishart, D. S., Sykes, B. D., and Richards, F. M. (1991) *J. Mol. Biol. 222* (2), 311−333.
55. Wishart, D. S., Sykes, B. D., and Richards, F. M. (1992) *Biochemistry 31*, (6), 1647−1651.
56. Wuthrich, K. (1986) *NMR of Proteins and Nucleic Acids*, Wiley, New York.
57. Searle, M. S., Zerella, R., Williams, D. H., and Packman, L. C. (1996) *Protein Eng. 9*, 559−565.
58. Walgers, R., Lee, T. C., and Cammers-Goodwin, A. (1998) *J. Am. Chem. Soc. 120*, 5073−5079.
59. Damaschun, G., Damaschun, H., Gast, K., and Zirwer, D. (1999) *J. Mol. Biol. 291*, 715−725.
60. Akke, M., and Forsen, S. (1990) *Proteins*: *Struct., Funct., Genet. 8*, 23−29.
61. Marqusee, S., and Sauer, R. T. (1994) *Protein Sci. 3*, 2217−2225.
62. Monera, O. D., Kay, C. M., and Hodges, R. S. (1994) *Protein Sci. 3*, 1984−1991.
63. Spolar, R. S., Livingstone, J. R., and Record, M. T., Jr. (1992) *Biochemistry 31*, 3947−3955.
64. Makhatadze, G. I., and Privalov, P. I. (1992) *J. Mol. Biol. 226*, 491−505.
65. Ramos, C. H. I., Kay, M. S., and Baldwin, R. L. (1999) *Biochemistry 38*, 9783−9790.
66. Pace, C. N., Laurents, D. V., and Thomson, J. A. (1990) *Biochemistry 29*, 2564−2572.
67. Shortle, D., and Meeker, A. K. (1986) *Proteins*: *Struct., Funct., Genet. 1*, 81−89.
68. Myers, J. K., Pace, C. N., and Scholtz, J. M. (1995) *Protein Sci. 4*, 2138−2148.
69. Vijay-Kumar, S., Bugg, C. E., Wilkinson, K. D., Vierstra, R. D., Hatfield, P. M., and Cook, W. J. (1987) *J. Biol. Chem. 262*, 6396−6399.
70. Shortle, D. (1996) *FASEB J. 10*, 27−34.
71. Osapay, K., Case, D. A. (1994) *J. Biomol. NMR 4*, 215−230.
72. Williams, D. H., Maguire, A. J., Tsuzuki, W., and Westwell, M. S. (1998) *Science 280*, 711−714.
73. Robertson, A. D., and Murphy, K. P. (1997) *Chem. Rev. 97*, 1251−1267.
74. Plaxco, K. W., Simons, K. T., and Baker, D. (1998) *J. Mol. Biol. 277*, 985−994.
75. Chiti, F., Taddei, N., White, P. M., Bucciantini, M., Magherini, F., Stefani, M., and Dobson, C. M. (1999) *Nat. Struct. Biol. 6*, 1005−1009.
76. Goldenberg, D. P. (1999) *Nat. Struct. Biol. 6*, 987−990.
77. Khorasanizadeh, S., Peters, I. D., Roder, H. (1996) *Nat. Struct. Biol. 3*, 193−205.

BI000718R